Chapter 5

Differential Scanning Calorimetry of Protein–Lipid Interactions

Olga Cañadas and Cristina Casals

Abstract

Differential scanning calorimetry (DSC) is a highly sensitive nonperturbing technique used for studying the thermodynamic properties of thermally induced transitions. Since these properties might be affected by ligand binding, DSC is particularly useful for the characterization of protein interactions with biomimetic membranes. The advantages of this technique over other methods consist in the direct measurement of intrinsic thermal properties of the samples, requiring no chemical modifications or extrinsic probes. This chapter describes the basic theory of DSC and provides the reader with an understanding of the capabilities of DSC instrumentation and the type of information that can be achieved from DSC studies of lipid–protein interactions. In particular, the chapter provides a detailed analysis of DSC data to assess the effects of proteins on biomimetic membranes.

Key words Differential scanning calorimetry, Lipids, Proteins, Lipid–protein interaction, Gel to liquid–crystalline phase transition, Lamellar to inverted hexagonal phase transition, Data analysis

1 Introduction

Differential scanning calorimetry (DSC) is a primary technique for measuring the energetics of thermally induced phase transitions and conformational changes, which makes DSC especially apt for investigating the thermodynamic properties of lipid/protein interactions.

DSC measures the heat that flows through a sample undergoing a physical transformation like a structural change or phase transition, in comparison to a reference material, when heated or cooled at identical, predetermined rates. Because of the absorption (or release) of heat from the sample during the thermal transition, a temperature differential (ΔT) develops between the sample and reference cells. The instrumental control system minimizes the temperature differential by supplying more (or less) heat to the

Jörg H. Kleinschmidt (ed.), *Lipid-Protein Interactions: Methods and Protocols*, Methods in Molecular Biology, vol. 2003, https://doi.org/10.1007/978-1-4939-9512-7_5,

sample cell to maintain its temperature equal to that of the reference cell. The thermal power required to maintain both cells at the same temperature is recorded and transformed in an output of heat capacity versus temperature.

1.1 Calorimeters

Based on the mechanism of operation, DSC instruments are classified into two types:

Heat-flux calorimeters: Sample material and reference (usually a buffer), enclosed in different pans, are in thermal contact with a heat flow sensor placed in a furnace. Both sample and reference cells are heated or cooled indirectly by contact with the furnace, which is heated or cooled at a linear heating rate (Fig. 1a). The heat released (or absorbed) during the calorimetric event is allowed to flow to (or from) the surrounding furnace. Because of the large time constant of the measurement system, it is necessary to operate at very slow scan rates to maintain thermal equilibrium.

Power compensation calorimeters: Sample and reference pans are placed in separated furnaces and are heated (or cooled) by independent heat sources (Fig. 1b). Both cells are maintained at the desired temperature by continuously manipulating the power supplied to an electrical heating element placed within the vessel, and the difference in thermal power required to maintain them at the same temperature is measured. These calorimeters have a very short response time and operate at considerably faster scanning rates than those of heat-flux instruments.

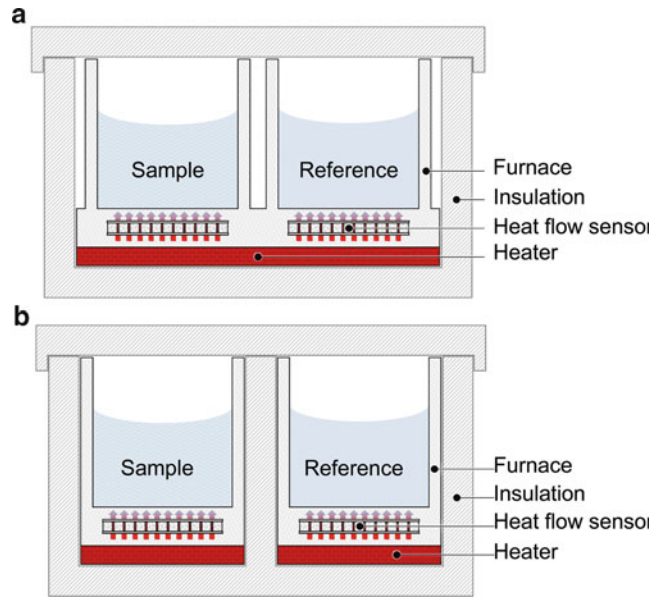

Fig. 1 Types of differential scanning calorimeters: (**a**) heat-flux calorimeter; (**b**) power compensation calorimeter

Modern DSC instruments are characterized by high sensitivity, a stable instrumental baseline, and a wide operational range, being able to scan aqueous solutions from 0 °C up to 100 °C. Some instruments are equipped with an automatic system that heats the cells to avoid the freezing of water, allowing supercooling of the sample below 0 °C. On the other hand, to heat the samples above 100 °C, DSC instruments are equipped with pressure-resistant sample cells that allow application of an excess pressure of 2 atm. to dissolve bubbles forming in the solution upon heating. Replacement of coin-shaped pans for capillary tubes allows calorimeters such as the Nano DSC to operate with very small sample quantities (300 μL, 2 μg protein). Automated cell filling and cleaning devices recently incorporated in many DSC models enable computer-controlled sample addition and data analysis.

1.2 Lipid Thermotropic Phase Behavior

Figure 2 shows the typical DSC thermogram for the first-order gel (L_β) to liquid–crystalline (L_α) phase transition exhibited by an aqueous dispersion of multilamellar vesicles of a single phospholipid (*see* **Note 1**). The thermodynamic parameters that characterize the phase transition, that is, the phase transition temperature (T_m), the relative cooperativity of the phase transition, and the enthalpy of the calorimetric event (ΔH), can be directly determined from the thermogram. The phase transition temperature, T_m, for lipid hydrocarbon chain-melting transitions is the maximum excess specific heat absorbed by the system [1–3]. Lipid samples that have attained thermodynamic equilibrium exhibit symmetric DSC traces (*see* **Note 2**). For these samples T_m represents the temperature at which the gel to liquid–crystalline phase transition is half complete [2, 4]. Below the onset temperature (T_s) the membrane is in the gel state, and above the completion temperature (T_C) the sample is in

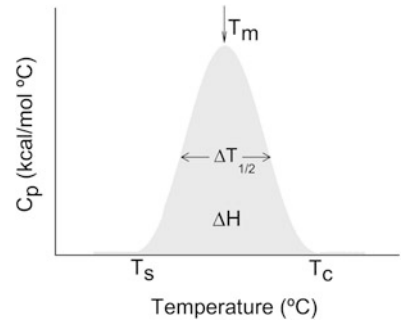

Fig. 2 DSC heating thermogram for the gel to liquid–crystalline endothermic phase transition of a pure phospholipid at equilibrium. The phase transition is characterized by the following thermodynamic parameters: T_m, the phase transition temperature; ΔH, the enthalpy of the calorimetric event; $\Delta T_{1/2}$, the transition width at half-height; T_s, the effective starting temperature of the transition; T_c, the completion temperature of the transition

the liquid crystalline phase, whereas lipids in the gel and fluid phases coexist at any point under the transition endotherm.

The cooperativity of the gel to liquid–crystalline phase transition is related to the reorganization of lipid molecules, which move in consort with each other, gaining new motional freedom. Near the phase transition temperature the membrane behaves as a composite material with fluid domains interspersed in the gel phase. The average number of lipid molecules in these fluid domains, that is, the number of lipid molecules involved in the transition, is called the cooperative unit (CU). CU reaches a zero value for noncooperative processes, whereas large values of CU indicate high cooperativity [1]. Since the highly correlated molecular motion in the cooperative unit facilitates the change of order at the phase transition temperature, the larger the cooperative unit, the narrower the temperature range of the phase transition. The sharpness of the transition peak is given by the temperature width at half-height, $\Delta T_{1/2}$, of the DSC trace. $\Delta T_{1/2}$ values can range from less than 0.1 °C for pure single lipids to 10–15 °C for complex lipid mixtures [1–3]. This broadening of the phase transition is due to the limited cooperativity of the transition. The dependence of $\Delta T_{1/2}$ on lipid–lipid interactions makes this parameter a valuable tool to estimate purity, protein–lipid interactions, as well as lipid-lipid interactions.

The enthalpy of the endothermic or exothermic event is evaluated by the integration of the area of the scan rate-normalized DSC peak relative to the experimental baseline [1, 2, 5]. The enthalpy of the gel to liquid–crystalline phase transition depends on the structure of the lipid, especially on the length of the fatty acid chain and the degree of unsaturation [1, 6]. In mixed-chain phospholipids, with *sn*1-saturated and *sn*2-unsaturated acyl chains, the presence of a single double bond into the *sn*2-acyl chain phospholipid lowers its phase transition temperature and ΔH. The placement of this double bond near the center of the *sn*2-acyl chain resulted in maximal reduction of the transition temperature and ΔH [6]. However, ΔH values increase as *sn*-2 unsaturation continues beyond three double bonds to the maximally nonconjugated cis-unsaturated state (i.e., 20:5*n*3 and 22:6*n*3, for the 20 and 22 carbon length chains, respectively) [6]. Stronger van der Waals interactions between neighboring *sn*-1-saturated chains would predictably increase ΔH values [6].

In addition to the gel to liquid–crystalline lamellar phase transition, lipids can undergo other phase transitions like the pretransition from a gel to a rippled gel ($P_{\beta'}$) phase of disaturated phosphatidylcholines and the lamellar to inverted hexagonal (H_{II}) phase transition of unsaturated phospholipids that contain small, strongly interacting polar headgroups such as phosphatidylethanolamines (Fig. 3) (*see* **Note 3**). Since these transitions are kinetically controlled, approaching the thermodynamic equilibrium at a slower rate than the temperature scanning rate, both the shape

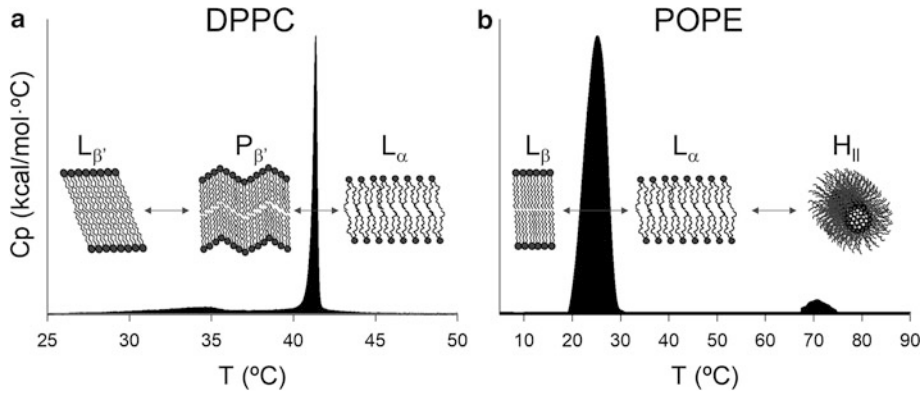

Fig. 3 DSC thermograms for (**a**) the $L_{\beta'}/P_{\beta'}$ and $P_{\beta'}/L_{\alpha}$ phase transitions of DPPC and (**b**) the L_{β}/L_{α} and L_{α}/H_{II} phase transitions of POPE. The $P_{\beta'}/L_{\alpha}$ and the L_{β}/L_{α} phase transitions are more energetic than the $L_{\beta'}/P_{\beta'}$ and L_{α}/H_{II} phase transitions. Disruption of the acyl chain interactions between adjacent lipid molecules that give rise to the gel to liquid–crystalline phase transition requires an energy supply. However, for the $L_{\beta'}/P_{\beta'}$ and L_{α}/H_{II} phase transitions the interactions between adjacent acyl chains are not affected and consequently, less energy is required for the phase transition

and the transition temperature of the phase transition are affected by the scanning rate. Therefore, slow scanning rates should be used to obtain reliable data on the enthalpy of these processes.

1.3 Theory

Differential scanning calorimetry measures the excess heat capacity, C_p, of the sample solution with respect to the reference material, which is usually the same buffer used in the preparation of the sample solution. The calorimetric enthalpy, ΔH_{cal}, and the entropy of the transition are related to the heat uptake involved in the heating process. ΔH_{cal} can be determined by integrating the DSC peak:

$$\Delta H_{\text{cal}} = \int C_p \cdot \mathrm{d}T \tag{1}$$

and the entropy of the transition is given by

$$\Delta S = \frac{\Delta H_{\text{cal}}}{T_{\text{m}}} \tag{2}$$

where T_{m} is the transition temperature.

The standard free energy change that occurs during the transition, ΔG^0, quantifies the stability of biological macromolecules and biomolecular associations. At equilibrium, ΔG^0 is related to the equilibrium constant, K, between the two states by

$$\Delta G^0 = -RT \ln K \tag{3}$$

where T is the absolute temperature and R is the universal gas constant. ΔG^0 is the sum of the enthalpy (ΔH^0) and entropy (ΔS^0) changes at the temperature at which ΔG^0 is evaluated:

$$\Delta G^0 = \Delta H^0 - T\Delta S^0 \tag{4}$$

ΔH^0, also known as the van't Hoff enthalpy (ΔH_{vH}), can be obtained by noncalorimetric methods from the change in the equilibrium constant value with temperature given by the van't Hoff equation for a simple two-state transition:

$$\left(\frac{\partial \ln K}{\partial T}\right)_p = \frac{\Delta H_{\mathrm{vH}}}{RT^2} \tag{5}$$

If ΔH^0 is independent of the temperature, a plot of the natural logarithm of K versus $1/T$ gives a straight line, the slope of which is $-\Delta H^0/R$.

$$\ln K = -\frac{\Delta H^0}{RT} + \frac{\Delta S^0}{R} \tag{6}$$

This plot is linear only in certain simple cases and over relatively narrow ranges of temperature. In general, ΔH^0 is temperature dependent, and a curvature of the van't Hoff plot is observed. In this case, it is necessary to subject the data to nonlinear least squares analysis employing the integrated form of the van't Hoff equation [7]:

$$\ln\frac{K}{K_0} = \frac{\Delta H_0 - T_0\Delta C_p}{R}\left(\frac{1}{T_0} - \frac{1}{T}\right) + \frac{\Delta C_p}{R}\ln\frac{T}{T_0} \tag{7}$$

where T_0 is an arbitrarily selected reference temperature, and K_0 is the equilibrium constant at that temperature.

The ratio of $\Delta H_{\mathrm{vH}}/\Delta H_{\mathrm{cal}}$ gives the number of molecules (or moles) per cooperative unit (*see* **Note 4**). Protein effects on the cooperativity of the phase transition of biomimetic membranes can be evaluated by comparing the *CU* values for phospholipid bilayers in the absence and presence of different amounts of reconstituted protein.

2 Materials

2.1 Equipment

1. DSC instrument (MicroCal PEAQ-DSC, TA Instruments NanoDSC, PerkinElmer DSC 4000, or equivalent).
2. Degassing equipment (vacuum desiccator, magnetic stirrer).
3. Dialysis tubing or cassettes (e.g., Pierce Slide-A-Lyzer Dialysis Cassettes).
4. Polystyrene beads (e.g., Sigma-Aldrich Amberlite XAD-25 or XAD-2, SM2 Bio-Beads).
5. Gel filtration columns (e.g., Sephadex G-50 or Seperdex 200).
6. Centrifuge (Beckman Optima XL-90, or equivalent).

2.2 Reagents

1. *Buffer*: Buffers with a small or zero enthalpy of ionization and pKa values that do not vary as a function of temperature like acetate, phosphate, formate, and Pipes are suitable for DSC measurements. If divalent metals are required for maintaining molecular stability, Ca^{2+} should be substituted for Mg^{2+} when working with phosphate buffer since Mg^{2+} creates baseline artifacts. Reducing agents like β-mercaptoethanol should be avoided because of oxidation and thermal degradation. The pH and ionic strength of the buffer solution should be chosen to avoid sample aggregation (*see* **Note 5**). Although the choice of buffer depends on the type of study, the buffer most widely used to study lipid-protein interactions is 10 mM HEPES, 0.1 mM NaCl, pH 7.4.
2. *Organic solvents*: Usually, a chloroform/methanol mixture is used to dissolve the lipids. When the reconstitution of hydrophobic membrane proteins into proteoliposomes is performed by codissolving lipids and protein in organic solvents, the chosen solvents should affect neither the structure nor the function of the protein.
3. *Detergent*: For protein reconstitution into proteoliposomes, mild detergents that preserve the native biological structure and activity of the proteins like octylglucoside, CHAPS, or Triton X-100 should be used. Sodium cholate is suitable for preparing lipid nanodiscs.
4. *Sample*: The lipid component should exhibit phase transition temperatures below the thermal denaturation temperature of the protein of interest (*see* **Note 6**).

3 Methods

3.1 Sample Preparation

Reliable DSC data of lipid–protein interactions require successful reconstitution of membrane proteins. Therefore, we present the various strategies commonly used to reconstitute proteins into liposomes and lipid bilayer nanodiscs.

Only the purest lipid and protein samples should be used in lipid-protein interaction studies.

1. *Preparation of proteoliposomes*: Proteoliposomes, phospholipid vesicles that contain integral membrane proteins, are an excellent tool for studying protein effects on the physical properties of membranes as well as the structure and function of membrane proteins. Among the different strategies developed for reconstitution of integral protein membranes into liposomes, the most successful and widely used strategy is the detergent-mediated protein pathway, which involves the transfer of an integral membrane protein from a detergent solution to

phospholipid vesicles [8, 9]. In the simple dilution approach the detergent-solubilized protein is diluted in a liposome solution and, when the concentration of detergent falls below its critical micelle concentration (CMC), the protein transfers into the liposome. Detergents with high CMCs that form small micelles (like cholate or CHAPS) are easily removed by dialysis or gel-filtration techniques, while detergents with high CMCs that form large micelles (Triton X-100) can be efficiently removed through adsorption on hydrophobic resins such as SM2 Bio-Beads or Amberlite XAD. Large proteoliposomes of extremely hydrophobic proteins can be formed by evaporating the apolar organic solvent in which lipids and proteins have been codissolved followed by rehydration with an aqueous buffer. Proteoliposomes are separated from plain bilayers and amorphous material by density gradient centrifugation.

2. *Proteoliposome characterization*: Since the conditions of proteoliposome preparation may affect the mode and extent of interaction of membrane proteins with liposomes [10], proteoliposomes should be thoroughly characterized prior to the DSC study to achieve optimal reconstitution and avoid artifactual interpretation of the results. Besides evaluating the integrity and activity of the protein under study, it is necessary to determine the morphology and size of the proteoliposomes, the homogeneity of protein distribution, the number of protein units incorporated, and the orientation of the incorporated protein [9]. The presence of residual solvents or detergents in the sample should also be checked (*see* **Note 7**).
3. *Generation of nanodiscs*: The generation of nanodiscs implies the self-assembly of the phospholipids, the protein of interest, and the membrane scaffold protein (MSP) from a detergent micellar state (*see* **Note 8**). Plain nanodiscs are generated by hydration of a dried lipid film of DPPC, DMPC, or POPC with a sodium-cholate-containing buffer, followed by sample sonication and incubation with an MSP solution. Nanodisc self-assembly is started upon removal of the detergent. Generally, this process is performed using beads like XAD-2. For incorporation of membrane target proteins, the mixture of phospholipids, sodium cholate, and MSP is incubated with the detergent-solubilized protein target on ice and subsequent detergent removal. To separate empty nanodiscs from protein-containing discs, size-exclusion chromatography or affinity chromatography is used.
4. *Sample concentration*: To obtain the best quantitative results, lipid and protein concentrations should be accurately determined, preferably by phosphorous determination and absorbance measurements at 280 nm, respectively. Alternatively, lipid concentration can be assessed by inclusion of trace

quantities of ^{14}C lipids in the reconstitution mixture followed by liquid scintillation counting of the reconstituted proteoliposomes.

5. *Sample degassing*: Bubble formation in the calorimetric vessel affects the accuracy of the volume and adds experimental noise to the thermograms [11, 12]. Therefore, it is necessary to degas under vacuum with gentle stirring of both the sample and reference solutions before starting the measurement (*see* **Note 9**).

3.2 DSC Procedure

1. *Loading the calorimeter*: Load the degassed buffer solution into the sample and reference cells and collect several scans until the baseline stabilizes (*see* **Note 10**). Allow the DSC cells to cool to approximate room temperature and, without stopping scanning, replace the solvent in one of the calorimetric cells with the sample solution. This minimizes baseline artifacts induced by the thermal shock involved in loading the sample or reference cells.
2. *Recording the DSC scan*: It is essential to determine the reversibility of the phase transition before extracting thermodynamic properties from the data (*see* **Note 11**). To obtain comparable results during a series of related experiments, sample scanning must be performed using the same parameters employed for determining the baseline: equilibration prior to the run, scan rate, starting and final temperatures, filtering period, gain, cool-down, and reequilibration. For pure lipids that exhibit a sharp transition, very low scan rates (around 0.1 K/min or less), filter periods of 1–5 s, and high gain feedback are usually appropriate.
3. *Cleaning the calorimeter*: To ensure reliable data, sample and reference cells must be clean. For samples that do not precipitate/aggregate, cells can be rinsed with water between different sample scans. If precipitation/aggregation occurs, the sample cell must be cleaned with a dilute detergent such as 1% Contrad®, followed by a water rinse. More thorough cleaning can be performed with nitric or formic acid. Once the cleaning procedure has finished, it is necessary to ascertain correct cleaning by loading the system with water and running baseline scans overnight.

3.3 Data Analysis

1. *Reference subtraction*: Since protein and lipid molecules have lower specific heat than water, it is necessary to subtract the heat capacity of the buffer to obtain the excess differential heat capacity contribution arising from the process of interest.
2. *Baseline subtraction*: The instrument baseline, which represents the residual heat flow signal of the DSC when operated empty,

affects both the area under the thermograms and the shape of the phase transition and hence, the estimation of both calorimetric and van't Hoff enthalpies. Therefore, to obtain reliable DSC data it is necessary to subtract the instrumental baseline from the sample trace. To facilitate estimation of the behavior of the baseline in the region under the endotherm in the absence of the transition, the temperature range scanned during a DSC assay should be broad enough for the instrument to establish stable baselines before and after the transition peak. The software of the calorimeter provides different baseline approaches like the progress, step, linear, or quadratic interpolations of pre-and posttransition baselines. All these baseline approaches should be checked to elucidate the uncertainties in ΔH_{cal} and ΔH_{vH} derived from each baseline type (*see* **Note 12**).

3. *Data deconvolution*: The calorimetric enthalpy, entropy, and often heat capacity changes for the overall transition are directly observable from the experimental melting curve. However, it is necessary to deconvolute the DSC data using a simple 2-state model to obtain the thermotropic parameters T_m and $\Delta T_{1/2}$. In addition, deconvolution of thermal transitions of membrane-embedded proteins allows determination of the character of the unfolding process [13].

3.4 Data Interpretation

The ability of DSC to monitor protein unfolding and lipid phase transitions has converted this technique in a valuable tool to study lipid–protein interactions [14]. DSC allows determination of the interaction mechanism of proteins and peptides with lipid bilayers that mimic eukaryotic and bacterial membranes, and provides information about the stability of membrane-embedded proteins.

Generally, protein incorporation in membranes composed of one lipid species broadens the gel to liquid–crystalline phase transition, with a concomitant change of ΔH and a shift of T_m relative to that of the pure lipid membrane. Protein effects on the phase behavior of phospholipid membranes allow determination of the lipid–protein interaction mechanism [15]. Thus, hydrophilic proteins that interact with the bilayer surface through electrostatic forces do not expand phospholipid monolayers nor alter the permeability of phospholipid vesicles into which they are interacting. Consequently, these proteins produce no change or a slight increase in the T_m and the $\Delta T_{1/2}$ of the transition, and a substantial increase in ΔH in a dose-dependent manner. Because of the electrostatic nature of the lipid–protein interaction, protein effects on negatively charged phospholipids are stronger than on zwitterionic phospholipids. On the other hand, peripheral proteins that initially adsorb to the charged polar head groups of the phospholipids and then partially penetrate the hydrophilic–hydrophobic interface of the bilayer decrease van der Waals interactions between lipid acyl

chains. As a result, T_m and/or ΔH decrease. These proteins normally expand phospholipid monolayers and alter the permeability of phospholipid vesicles into which they are incorporated. Finally, hydrophobic integral membrane proteins have little effect on T_m, but reduce the cooperativity of gel to liquid–crystalline phase transitions and decrease ΔH usually linearly, with increasing protein concentrations. These effects are due to deep protein penetration into the hydrophobic core of the membrane, which prevents some lipid molecules from participating in the melting transition. The number of phospholipid molecules that do not participate in the transition can be determined from the dependence of the transition enthalpy on the protein–lipid molar ratio [16]:

$$\Delta H = \Delta H_0 \cdot \left[1 - m \cdot \frac{P}{L}\right] \tag{8}$$

where ΔH_0 and ΔH are the transition enthalpies in the absence and presence of protein, respectively; P/L is the protein–lipid molar ratio; and m is the number of phospholipid molecules prevented from participating in the gel to liquid–crystalline phase transition by one molecule of protein (*see* **Note 13**).

Protein-induced changes in the transition temperature and shape of the DSC peaks also provide information on the miscibility of lipids and proteins. Thus, proteins that ideally mix with both lipid phases symmetrically broaden the DSC curve [17]. Conversely, proteins that do not bind well with both lipid phases slightly affect the transition by aggregating into clusters at all temperatures, thus reducing its interface with the lipids. Proteins that mix well with the gel phase increase the T_m and broaden the high-temperature side of the transition, whereas proteins that mix well with fluid phase lipids shift the DSC curve to lower temperatures and broaden the low-temperature side of the transition. The decrease of the T_m induced by the protein, that is, the van't Hoff freezing point depression, can be estimated by the following equation:

$$\Delta T_m = -\left(\frac{RT_m^2}{\Delta H}\right)X \tag{9}$$

where ΔH is the transition enthalpy of the lipid bilayers, R the universal gas constant, T_m the transition temperature, and X the molar fraction of the protein or peptide incorporated into the membrane. In the case of nonideal mixing:

$$\Delta T_m = -\left(\frac{RT_m^2}{\Delta H}\right)X(1 - wX) \tag{10}$$

where w is the nonideal mixing parameter.

Strong lipid–protein interactions can result in the formation of domains within lipid membranes, especially if the proteins have a high affinity for a particular lipid component. Integral membrane

proteins induce the formation of lipid domains by direct interaction with the surrounding lipids, oligomerization, or hydrophobic matching [18]. Peripheric proteins promote lipid segregation by electrostatic interaction with lipid headgroups [19]. Enrichment of a particular lipid component in one region of the membrane results in a sharper transition and increased enthalpy for this particular lipid. As a result, shoulders or double peaks appear in the DSC trace [19, 20].

Proteins and peptides can modulate the tendency of lipids to form nonlamellar phases. Induction of curvature strain affects the stability of the membrane and is involved in pore formation by antimicrobial peptides, membrane fusion, translocation of antimicrobial peptides across the bacterial membrane, or cell toxicity of amyloidogenic peptides. DSC experiments with non-bilayer-forming lipids such as phosphatidylethanolamines have been performed to assess the curvature stress exerted on the membrane (Fig. 3). These phospholipids spontaneously form lipid bilayers in the liquid–crystalline state below the L_α–H_{II} transition temperature, T_H, whereas above T_H, they pack in a highly curved hexagonally inverted structure with negative membrane curvature (Fig. 3) [21]. Shift of T_H is an excellent indicator of curvature alterations. Stabilization of the H_{II} phase due to protein binding decreases the T_H, whereas proteins that induce positive membrane curvature increase T_H, stabilizing the liquid crystalline bilayer phase.

Although in the context of lipid–protein interactions DSC is mainly used to characterize the perturbations of the thermotropic properties of lipid bilayers induced by proteins, this technique can also be used to evaluate the effect of lipid composition on protein stability. Membrane protein folding consists of a four-step pathway: partitioning, folding, insertion, and association [22]. Determination of ΔG^0 for each step allows the thermodynamic stabilities to be ascertained.

4 Notes

1. Multilamellar vesicles are generally used for DSC studies since they provide the clearest resolution of the phase transitions [5, 23]. The smaller radius of small unilamellar vesicles (SUVs) over MLVs decreases lipid order, which increases the free motion of the hydrocarbon chains [1]. As a result, the transitions broaden and become less enthalpic, and no pretransitions are observed. For large unilamellar vesicles (LUVs) the thermograms are nearly identical to those of MLVs, although size inhomogeneity slightly broadens the endotherms [5]. Loss of cooperativity has also been observed in lipid nanodiscs [24]. This effect has been attributed to the small size of the

nanodiscs and the interaction of boundary lipids with the MSP protein encircling the discs.

2. In many lipid mixtures the phase transition does not proceed under equilibrium conditions. This results in asymmetric DSC curves, and the T_m and the phase transition midpoint temperature do not coincide [1].
3. These thermotropic interconversions have a much lower enthalpy than the gel to liquid–crystalline phase transition, and hence high lipid concentrations and high sensitivity DSC instruments are required for a proper measurement of the transition.
4. CU values can be affected by the presence of impurities of incorrect concentration estimates that give rise to errors in ΔH_{cal} and, consequently, in $\Delta H_{vH}/\Delta H_{cal}$ ratios.
5. Sample aggregation makes data unusable by causing a rapid downward shift and/or an increase in baseline noise. It is possible to reduce sample aggregation by decreasing the concentration, changing the pH, and/or using a different buffer. In addition, sample precipitation can damage the instrument. Therefore, sample precipitation must be tested before performing the measurement by incubating a small fraction of the sample at the experimental temperature for 1 h.
6. To model eukaryotic cell membranes, lipid–protein interactions are usually studied by employing disaturated phosphatidylcholines since these phospholipids are stable to oxidation, hydrate readily, and form lamellar phases at physiological temperatures in excess water [2]. However, lipid mixtures should be used to characterize the preferential interaction of a protein with a certain lipid component or the role of lipid bilayer fluidity and electrostatic interactions in the lipid-protein interaction. When designing a lipid mixture, it is necessary to consider the miscibility of the lipids since not all the lipids are miscible.
7. The thermodynamic properties of the reconstituted lipoprotein complexes can be affected by alterations in lipid size and homogeneity of the proteoliposomes or detergent or solvent traces [1]. In addition, the exposure of membrane proteins to organic solvents may denature the proteins. On the other hand, it is necessary to control the final orientation of the protein in the proteoliposomes since disorientation of the protein causes aggregation, which may affect the interaction of the protein with the membrane.
8. For successful nanodisc construction, it is critical to have the correct stoichiometry of phospholipids, target protein, and MSP. The phospholipid–MSP ratio depends on the particular phospholipid and MSP, being higher for disaturated than for

unsaturated phosphatidylcholines. This ratio must be adjusted when assembly is done at low MSP/target protein ratios. Cholate concentration should be twice the lipid concentration to facilitate nanodisc assembly. The choice and concentration of the detergent used for solubilizing the target protein depends on the particular membrane protein and must be determined empirically. On the other hand, nanodisc assembly should be performed at a temperature close to the lipid melting temperature. Therefore, when using POPC the assembly should be conducted on ice. To accommodate different membrane proteins, it is possible to modify the diameter of the bilayer disc by using membrane scaffold proteins with varying lengths of the amphipathic helical region.

9. To decrease the amount of air dissolved in the buffer solution, the sample should be equilibrated at room temperature before degassing. Stirring the sample while degassing reduces the time required to completely degas the sample and reference solutions. Alternatively, to remove air bubbles that are difficult to eliminate, samples can de degassed by sonication.
10. To generate a reproducible baseline buffer scan, it is necessary to condition the sample cell during the first scan. To that end, sample and reference cells must be loaded with buffer and during the scan, buffer ions will adsorb onto the cell surface. The conditioning buffer should be replaced by fresh buffer in both cells for the subsequent scans.
11. Analysis of DSC data by equilibrium thermodynamics-based approaches requires equilibrium data. The equilibrium criterion usually applied is the reproducibility of the sample DSC trace in a second heating.
12. In case of baseline uncertainty, it is possible to obtain a weight average enthalpy estimate close to the true value by applying the following equation [25]:

$$\Delta H_{\mathrm{WA}} = 0.65\Delta H_{\mathrm{vH}} + 0.35\Delta H_{\mathrm{cal}} \tag{12}$$

This empirical formula should not be applied when differences in van't Hoff and calorimetric enthalpies are not due to poor baseline correction.

13. Positive deviations of linearity indicate that either the protein aggregates within the bilayers, decreasing the number of lipid molecules affected by the protein, or the interaction with the bilayer has been modified by changes in the conformation of the hydrophilic regions of the protein.

Acknowledgments

This work was supported by Spanish Ministry of Economy and Competitiveness (SAF2015-65307-R) and Institute of Health Carlos III (CIBERES CB06/06/0002).

References

1. McElhaney RN (1982) The use of differential scanning calorimetry and differential thermal analysis in studies of model and biological membranes. Chem Phys Lipids 30:229–259
2. McElhaney RN (1986) Differential scanning calorimetric studies of lipid-protein interactions in model membrane systems. Biochim Biophys Acta 864:361–421
3. Demetzos C (2008) Differential scanning calorimetry (DSC): a tool to study the thermal behavior of lipid bilayers and liposome stability. J Liposome Res 18:159–173
4. Lewis RN, Mannock DA, McElhaney RN (2007) Differential scanning calorimetry in the study of lipid phase transitions in model and biological membranes. In: Dopico AM (ed) Methods in membrane lipids. Methods in molecular biology™, vol 400. Humana Press, Totowa, NJ, pp 171–195
5. Biltonen RL, Lichtenberg D (1993) The use of differential scanning calorimetry as a tool to characterize liposome preparations. Chem Phys Lipids 64:129–142
6. Niebylski CD, Salem NJ (1994) A calorimetric investigation of a series of mixed-chain polyunsaturated phosphstidylcholines: effect of sn-2 chain length and degree of unsaturation. Biophys J 67:2387–2393
7. Naghibi H, Tamura A, Sturtevant JM (1995) Significant discrepancies between van't Hoff and calorimetric enthalpies. Proc Natl Acad Sci U S A 92:5597–5599
8. Seddon AM, Curnow P, Booth PJ (2004) Membrane proteins, lipids and detergents: not just a soap opera. Biochim Biophys Acta 1666:105–117
9. Rigaud JL, Pitard B, Levy D (1995) Reconstitution of membrane proteins into liposomes: application to energy-transducing membrane proteins. Biochim Biophys Acta 1231:223–246
10. Cruz A, Casals C, Keough KM et al (1997) Different modes of interaction of pulmonary surfactant protein SP-B in phosphatidylcholine bilayers. Biochem J 327:133–138
11. Privalov PL, Dragan AI (2007) Microcalorimetry of biological macromolecules. Biophys Chem 126:16–24
12. Privalov PL, Potekhin SA (1986) Scanning microcalorimetry in studying temperature-induced changes in proteins. In: Hirs C, Timasheff S (eds) Enzyme structure, Part L, vol 131. Academic Press, Orlando, FL, pp 4–51
13. Spink CH (2015) The deconvolution of differential scanning calorimetry unfolding transitions. In: Chaires JB, Hansen LD, Keller S, Brautigam CA, Zhao H, Schuck P (eds) Biocalorimetry. Methods, vol 76. Elsevier, Amsterdam, pp 78–86
14. Cañadas O, Casals C (2013) Differential scanning calorimetry of protein-lipid interactions. In: Kleinschmidt J (ed) Lipid-protein interactions. Methods in molecular biology (Methods and protocols), vol 974. Humana Press, Totowa, NJ, pp 55–71
15. Papahadjopoulos D, Moscarello M, Eylar EH et al (1975) Effects of proteins on thermotropic phase transitions of phospholipid membranes. Biochim Biophys Acta 401:317–335
16. van Zoelen EJ, van Dijck PW, de Kruijff B et al (1978) Effect of glycophorin incorporation on the physico-chemical properties of phospholipid bilayers. Biochim Biophys Acta 514:9–24
17. Gómez-Fernández JC, Goñi FM, Bach D et al (1979) Protein—lipid interactions. A study of (Ca2+-Mg2+)ATPase reconstituted with synthetic phospholipids. FEBS Lett 98:224–228
18. Poveda JA, Fernández AM, Encinar JA et al (2008) Protein-promoted membrane domains. Biochim Biophys Acta 1778:1583–1590
19. Sáenz A, Cañadas O, Bagatolli LA et al (2006) Physical properties and surface activity of surfactant-like membranes containing the cationic and hydrophobic peptide KL4. FEBS J 273:2515–2527
20. Plasencia I, Cruz A, Lopez-Lacomba JL et al (2001) Selective labeling of pulmonary surfactant protein SP-C in organic solution. Anal Biochem 296:49–56

21. Siegel DP, Epand RM (1997) The mechanism of lamellar-to-inverted hexagonal phase transitions in phosphatidylethanolamine: implications for membrane fusion mechanisms. Biophys J 73:3089–3111
22. White SH, Wimley WC (1999) Membrane protein folding and stability: physical principles. Annu Rev Biophys Biomol Struct 28:319–365
23. Mason JT, Huang CM, Biltonen RL (1983) Effect of liposomal size on the calorimetric behavior of mixed-chain phosphatidylcholine bilayers dispersions. Biochemistry 22:2013–2018
24. Shaw AW, McLean MA, Sligar SG (2004) Phospholipid phase transitions in homogeneous nanometer scale bilayer discs. FEBS Lett 556:260–264
25. Haynie DT, Freire E (1994) Estimation of the folding/unfolding energetics of marginally stable proteins using differential scanning calorimetry. Anal Biochem 216:33–41